Structural Monitoring and Maintenance, *Vol. 6, No. 3 (2019) 191-218*
DOI: https:// doi.org/10.12989/smm.2019.6.3.191

Plane wave propagation in transversely isotropic magneto-thermoelastic rotating medium with fractional order generalized heat transfer

Parveen Lata and Iqbal Kaur*

Department of Basic and Applied Sciences, Punjabi University, Patiala, Punjab, India

(Received May 4, 2019, Revised August 25, 2019, Accepted August 27, 2019)

Abstract. The aim of the present investigation is to examine the propagation of plane waves in transversely isotropic homogeneous magneto thermoelastic rotating medium with fractional order heat transfer. It is found that, for two dimensional assumed model, there exist three types of coupled longitudinal waves (quasi-longitudinal, quasi-transverse and quasi-thermal waves). The wave characteristics such as phase velocity, attenuation coefficients, specific loss, penetration depths, energy ratios and amplitude ratios of various reflected and transmitted waves are computed and depicted graphically. The conservation of energy at the free surface is verified. The effects of rotation and fractional order parameter by varying different values are represented graphically.

Keywords: thermoelastic; transversely isotropic; magneto-thermoelastic rotating medium; fractional-order heat transfer; plane wave propagation

1. Introduction

The medium which deforms due to thermal shock and application of the magnetic field, produces an induced magnetic and electric field. The composite materials such as magneto-thermoelastic material gained considerable importance since last decade because these materials show the coupling effect between magnetic and thermal fields. The study of plane wave propagation in a thermoelastic solid gained considerable importance, due to its applications in the area of geophysics, nuclear fields, and related topics. In last decade significant attention has been given in the area of plane thermoelastic and magneto-thermoelastic wave propagation in a medium.

Borejko (1996) deliberated the reflection and transmission coefficients for 3D plane waves in elastic media. Wu and Lundberg (1996) examined the problem of reflection and transmission of the energy of harmonic elastic waves in a bent bar. Marin (1997) had proved the Cesaro means of the kinetic and strain energies of dipolar bodies with finite energy. Sinha and Elsibai (1997) discoursed the reflection and refraction of thermoelastic waves at an interface of two semi-infinite media with two relaxation times. Ting (2004) explored a surface wave propagation in an anisotropic rotating medium. Othman and Song (2006, 2008) presented different hypotheses about

*Corresponding author, Ph.D., E-mail: bawahanda@gmail.com

http://www.techno-press.org/?journal=smm&subpage=7 ISSN: 2288-6605 (Print), 2288-6613 (Online)

magneto-thermo-elastic waves in homogeneous and isotropic medium. Kumar and Chawla (2011) discussed the plane wane propagation in anisotropic three-phase lag model and two-phase lag model. Deswal and Kalkal (2015) discussed the problem in a surface suffering a time-dependent thermal shock for thermo-viscoelastic interactions in a homogeneous, isotropic three-dimensional medium.

The reflection of plane periodic wave occurrence on the surface of generalized thermoelastic micropolar transversely isotropic medium is studied by Kumar and Gupta (2012) to calculate complex velocities of the four waves i.e., quasi-longitudinal displacement (qLD) wave, quasi-transverse displacement (qTD) wave, quasi- transverse microrotational (qTM) wave and quasi thermal (qT) waves from the complex roots of a quartic equation. Abouelregal (2013) had investigated the induced displacement, temperature, and stress fields in an infinite transversely isotropic boundless medium with cylindrical cavity due to a moving heat source and harmonically varying heat in reference to the linear theory of generalized thermoelasticity with a dual-phase lag model. Abd-alla and Alshaikh (2015) had discussed the effect of rotation and magnetic field on plane waves in transversely isotropic thermoelastic medium under the Green-Lindsay theory with two relaxation times of generalized thermoelasticity to show the presence of three quasi plane waves in the medium. Marin *et al.* (2013) have modelled a micro stretch thermoelastic body with two temperatures and eliminated divergences among the classical elasticity and research.

The effects of reflection and refraction are studied by Gupta (2015) at the boundary of elastic and a thermoelastic diffusion media, for plane waves by expanding the Fick law with dual-phase-lag diffusion model with delay times of both mass flow as well as potential gradient. Besides, Kumar *et al.* (2016) had depicted the effect of time and thermal and diffusion phase lags for axisymmetric heat supply in a ring by using Laplace and Hankel transform technique for dual-phase-lag model for transfer of heat and diffusion for upper and lower surfaces of the ring which were considered as traction free.

Youssef (2013, 2016) proposed for an elastic half-space a two-temperature model with constant elastic parameters and with generalized thermoelasticity without energy dissipation and also constructed a theory of thermoelasticity based on fraction order Duhamel-Neumann stress-strain relation in context of one temperature type and two-temperature types. Sharma and Kaur (2015) had investigated the transverse vibrations due to time-varying patch loads in homogenous, transversely isotropic, thermoelastic thin beams. However, Kumar *et al.* (2016) had explored of uncertainties due to thermomechanical sources (concentrated and distributed) using Laplace and Fourier transform technique in a transversely isotropic homogeneous thermoelastic rotating medium with magnetic effect, two temperature and by G–N with and without energy dissipation w.r.t. thermomechanical sources.

Othman *et al.* (2017) proposed a model for generalized magneto-thermoelasticity in an isotropic elastic medium rotating with uniform angular velocity and with two–temperature under the effect initial stress under LS (Lord–Shulman), GL (Green–Lindsay) and CT (coupled theory) theories of generalized thermoelasticity. Kumar and Kansal (2017) found reflected and refracted waves occurrence due to longitudinal and transverse waves incident implicitly at a plane interface between uniform elastic solid half-space and magneto-thermoelastic diffusive solid half-space with voids as a function of the angle of incidence and frequency of the incident wave. Maitya *et al.* (2017) presented plane wave propagation in a rotating elastic fiber-reinforced medium with magnetic and thermal fields under GN –I and II type theories. Bayones and Abd-Alla (2017) discussed 2D problem of thermoelasticity regarding thermoelastic wave propagation in a rotating medium under magnetic field and time-dependent heat source effects due to thermomechanical

source. Said (2017) investigated the effect of hydrostatic initial stress and the gravity field on a thermoelastic medium which is fiber-reinforced with its own heat and constant motion by three-phase-lag model and GN Type II theory. Marin *et al.* (2017) studied the GN-thermoelastic theory for a dipolar body using mixed initial BVP and proved a result of Hölder's-type stability. Lata (2018a, b) studied the effect of energy dissipation on plane waves in sandwiched layered thermoelastic medium of uniform thickness, with combined effects of two temperature, rotation, and Hall current in the context of GN Type-II and Type-III theory of thermoelasticity. Ezzat and El-Bary (2017) gave mathematical model of phase-lag, GN, magneto-thermoelasticity theories for perfectly conducting media based on fractional derivative heat transfer in the presence of a constant magnetic field.

Alesemi (2018) demonstrated the efficiency of the thermal relaxation time depending upon LS theory, Coriolis and Centrifugal Forces on the reflection coefficients of plane waves in an anisotropic magneto-thermoelastic rotating with stable angular velocity medium. Othman *et al.* (2019) dealt with the deformation of an infinite micro stretch generalized thermoelastic rotating medium under the effects of initially applied magnetic and gravitational field in GN Theory of thermoelasticity. Despite of this several researchers worked on different theory of thermoelasticity as Marin (1994, 1999), Marin and Craciun (2017), Othman and Marin (2017), Hassan *et al.* (2018), Marin (1998, 2009, 2010), Lata *et al.* (2016), Lata and Kaur (2019a, b, c) and Lata and Kaur (2019d, e), Kaur and Lata (2019f).

Inspite of these, not much work has been carried out in plane wave propagation due to fractional order heat transfer in a transversely isotropic magneto thermoelastic medium. Keeping these considerations in mind wave propagation problem will be studied by using normal mode analysis & reflection techniques

2. Basic equations

The simplified Maxwell's linear equation of electrodynamics for a slowly moving and perfectly conducting elastic solid are

$$curl\,\vec{h} = \vec{j} + \varepsilon_0 \frac{\partial \vec{E}}{\partial t} \tag{1}$$

$$curl\,\vec{E} = -\mu_0 \frac{\partial \vec{h}}{\partial t} \tag{2}$$

$$\vec{E} = -\mu_0 \left(\frac{\partial \vec{u}}{\partial t} + \vec{H}_0 \right) \tag{3}$$

$$div\,\vec{h} = 0 \tag{4}$$

Maxwell stress components (Kumar *et al.* 2016) are given by

$$t_{ij} = \mu_0 (H_i h_j + H_j h_i - H_k h_k \delta_{ij}) \tag{5}$$

The constitutive relations for a transversely isotropic thermoelastic medium are given by

$$t_{ij} = C_{ijkl}e_{kl} - \beta_{ij}T \tag{6}$$

Equation of motion as described by Schoenberg and Censor (1973) for a transversely isotropic thermoelastic medium rotating uniformly with an angular velocity $\mathbf{\Omega} = \Omega\boldsymbol{n}$, where $\mathbf{n}$ is a unit vector representing the direction of the axis of rotation and taking into account Lorentz force

$$t_{ij,j} + F_i = \rho\{\ddot{u}_i + (\Omega \times (\Omega \times \mathrm{u})_i + (2\Omega \times \dot{u})_i\} \tag{7}$$

where $F_i = \mu_0(\vec{j} \times \vec{H}_0)$ are the components of Lorentz force, $\vec{H}_0$ is the external applied magnetic field intensity vector, $\vec{j}$ is the current density vector, $\vec{u}$ is the displacement vector, μ_0 and ε_0 are the magnetic and electric permeabilities respectively and t_{ij} the component of Maxwell stress tensor. The terms $\mathbf{\Omega} \times (\mathbf{\Omega} \times \mathbf{u})$ and $2\mathbf{\Omega} \times \dot{\boldsymbol{u}}$ are the additional centripetal acceleration due to the time-varying motion and Coriolis acceleration respectively. The heat conduction equation following Youseff (2006, 2010) is

$$K_{ij}\left(1 + \frac{(\tau_t)^\alpha}{\alpha!}\frac{\partial^\alpha}{\partial t^\alpha}\right)\dot{T}_{,ji} + K^*_{ij}\left(1 + \frac{(\tau_v)^\alpha}{\alpha!}\frac{\partial^\alpha}{\partial t^\alpha}\right)T_{,ji} = \left(1 + \frac{(\tau_q)^\alpha}{\alpha!}\frac{\partial^\alpha}{\partial t^\alpha} + \frac{(\tau_q)^{2\alpha}}{2\alpha!}\frac{\partial^{2\alpha}}{\partial t^{2\alpha}}\right)\left[\rho C_E\ddot{T} + \beta_{ij}T_0\ddot{\mathrm{e}}_{ij}\right] \tag{8}$$

where

$$\begin{cases} 0 < \alpha < 1 \text{ for weak conductivity,} \\ \alpha = 1 \text{ for normal conductivity,} \\ 1 < \alpha \leq 2 \text{ for strong conductivity,} \end{cases}$$

$$\beta_{ij} = C_{ijkl}\alpha_{ij} \tag{9}$$

$$e_{ij} = \frac{1}{2}(u_{i,j} + u_{j,i}), \quad i,j = 1,2,3.$$

$$\beta_{ij} = \beta_i\delta_{ij}, \quad K_{ij} = K_i\delta_{ij}, \quad \text{i is not summed.} \tag{10}$$

Here $C_{ijkl}(C_{ijkl} = C_{klij} = C_{jikl} = C_{ijlk})$ are elastic parameters, β_{ij} is the thermal elastic coupling tensor, T is the absolute temperature, T_0 is the reference temperature, φ is the conductive temperature, t_{ij} are the components of the stress tensor, e_{ij} are the components of strain tensor, u_i are the displacement components, ρ is the density, C_E is the specific heat, K_{ij} is the materialistic constant, α_{ij} is the coefficient of linear thermal expansion, τ_0 is the relaxation time, which is the time required to maintain steady-state heat conduction in an element of volume of an elastic body when sudden temperature gradient is imposed on that volume element, δ_{ij} is the Kronecker delta, $\mathbf{\Omega}$ is the angular velocity of the solid, τ_t is the phase lag of heat flux, τ_v is the phase lag of temperature gradient, τ_q is the phase lag of thermal displacement, α is the fractional parameter.

3. Formulation and solution of the problem

We consider a homogeneous transversely isotropic magnetothermoelastic medium initially at a uniform temperature T_0, permeated by an initial magnetic field $\vec{H}_0 = (0, H_0, 0)$ acting along y-axis. The rectangular Cartesian co-ordinate system (x, y, z) having origin on the surface $(z = 0)$ with z-axis pointing vertically into the medium is introduced. In addition, we consider that

$$\boldsymbol{\Omega} = (0, \Omega, 0)$$

From the generalized Ohm's law (Kumar *et al.* 2016)

$$J_2 = 0$$

The density components $J_1$and J_3 are given as

$$J_1 = -\varepsilon_0 \mu_0 H_0 \frac{\partial^2 w}{\partial t^2} \tag{11}$$

$$J_3 = \varepsilon_0 \mu_0 H_0 \frac{\partial^2 u}{\partial t^2} \tag{12}$$

In addition, the equations of displacement vector *(u,v,w)* and conductive temperature φ for transversely isotropic thermoelastic solid

$$u = u(x, z, t), v = 0, w = w(x, z, t) and\ \varphi = \varphi(x, z, t) \tag{13}$$

Now using the transformation on Eqs. (1)-(3) following Slaughter (2002) Eqs. (7) and (8) with the aid of (11)-(13), yield

$$C_{11}\frac{\partial^2 u}{\partial x^2} + C_{13}\frac{\partial^2 w}{\partial x \partial z} + C_{44}\left(\frac{\partial^2 u}{\partial z^2} + \frac{\partial^2 w}{\partial x \partial z}\right) - \beta_1 \frac{\partial T}{\partial x} - \mu_0 J_3 H_0 = \rho\left(\frac{\partial^2 u}{\partial t^2} - \Omega^2 u + 2\Omega \frac{\partial w}{\partial t}\right) \tag{14}$$

$$(C_{13} + C_{44})\frac{\partial^2 u}{\partial x \partial z} + C_{44}\frac{\partial^2 w}{\partial x^2} + C_{33}\frac{\partial^2 w}{\partial z^2} - \beta_3 \frac{\partial T}{\partial z} - \mu_0 J_1 H_0 = \rho\left(\frac{\partial^2 w}{\partial t^2} - \Omega^2 w - 2\Omega \frac{\partial u}{\partial t}\right) \tag{15}$$

$$K_1\left(1 + \frac{(\tau_t)^\alpha}{\alpha!}\frac{\partial^\alpha}{\partial t^\alpha}\right)\frac{\partial^2 \dot{T}}{\partial x^2} + K_3\left(1 + \frac{(\tau_t)^\alpha}{\alpha!}\frac{\partial^\alpha}{\partial t^\alpha}\right)\frac{\partial^2 \dot{T}}{\partial z^2} + K_1^*\left(1 + \frac{(\tau_v)^\alpha}{\alpha!}\frac{\partial^\alpha}{\partial t^\alpha}\right)\frac{\partial^2 T}{\partial x^2} + K_3^*\left(1 + \frac{(\tau_v)^\alpha}{\alpha!}\frac{\partial^\alpha}{\partial t^\alpha}\right)\frac{\partial^2 T}{\partial z^2} = \left(1 + \frac{(\tau_q)^\alpha}{\alpha!}\frac{\partial^\alpha}{\partial t^\alpha} + \frac{(\tau_q)^{2\alpha}}{2\alpha!}\frac{\partial^{2\alpha}}{\partial t^{2\alpha}}\right)\left[\rho C_E \ddot{T} + T_0\left\{\beta_1 \frac{\partial \ddot{u}}{\partial x} + \beta_3 \frac{\partial \ddot{w}}{\partial z}\right\}\right] \tag{16}$$

and

$$t_{11} = C_{11}e_{11} + C_{13}e_{13} - \beta_1 T \tag{17}$$

$$t_{33} = C_{13}e_{11} + C_{33}e_{33} - \beta_3 T \tag{18}$$

$$t_{13} = 2C_{44}e_{13} \tag{19}$$

where

$$\beta_1 = (C_{11} + C_{12})\alpha_1 + C_{13}\alpha_3,$$

$$\beta_3 = 2C_{13}\alpha_1 + C_{33}\alpha_3,$$

To simplify the solution, mention below dimensionless quantities are used

$$x' = \frac{x}{L}, \quad z' = \frac{z}{L}, \quad u' = \frac{\rho c_1^2}{L\beta_1 T_0}u, \quad w' = \frac{\rho c_1^2}{L\beta_1 T_0}w, \quad t' = \frac{c_1}{L}t,$$

$$T' = \frac{T}{T_0}, t'_{11} = \frac{t_{11}}{\beta_1 T_0}, \ t'_{33} = \frac{t_{33}}{\beta_1 T_0}, t'_{31} = \frac{t_{31}}{\beta_1 T_0}, h' = \frac{h}{H_0}, \ \Omega' = \frac{\mathrm{L}}{C_1}\Omega \tag{20}$$

Making use of (20) in Eqs. (14)-(16), after suppressing the primes, yield

$$\frac{\partial^2 u}{\partial x^2} + \delta_4 \frac{\partial^2 w}{\partial x \partial z} + \delta_2\left(\frac{\partial^2 u}{\partial z^2} + \frac{\partial^2 w}{\partial x \partial z}\right) - \frac{\partial T}{\partial x} = \left(\frac{\varepsilon_0 \mu_0^2 H_0^2}{\rho} + 1\right)\frac{\partial^2 u}{\partial t^2} - \Omega^2 u + 2\Omega \frac{\partial w}{\partial t} \tag{21}$$

$$\delta_1 \frac{\partial^2 u}{\partial x \partial z} + \delta_2 \frac{\partial^2 w}{\partial x^2} + \delta_3 \frac{\partial^2 w}{\partial z^2} - \frac{\beta_3}{\beta_1}\frac{\partial T}{\partial z} = \left(\frac{\varepsilon_0 \mu_0^2 H_0^2}{\rho} + 1\right)\frac{\partial^2 w}{\partial t^2} - \Omega^2 w - 2\Omega \frac{\partial u}{\partial t} \tag{22}$$

$$\left[1 + \frac{C_1}{L}\frac{\tau_T^\alpha}{\alpha!}\frac{\partial^{\alpha+1}}{\partial t^{\alpha+1}}\right]\left[K_1 \frac{\partial^2}{\partial x^2} + K_3 \frac{\partial^2}{\partial z^2}\right] T + \left[1 + \frac{\tau_v^\alpha}{\alpha!}\frac{\partial^\alpha}{\partial t^\alpha}\right]\left[K_1^* \frac{\partial^2}{\partial x^2} + K_3^* \frac{\partial^2}{\partial z^2}\right] T = \left[1 + \frac{\tau_q^\alpha}{\alpha!}\frac{\partial^\alpha}{\partial t^\alpha} + \frac{\tau_q^{2\alpha}}{2\alpha!}\frac{\partial^{2\alpha}}{\partial t^{2\alpha}}\right]\left[C_1^2 \rho C_E \ddot{T} + \beta_1 T_0 \left(\beta_1 \frac{\partial \ddot{u}}{\partial x} + \beta_3 \frac{\partial \ddot{w}}{\partial z}\right)\right] \tag{23}$$

where

$$\delta_1 = \frac{c_{13} + c_{44}}{c_{11}}, \qquad \delta_2 = \frac{c_{44}}{c_{11}}, \qquad \delta_3 = \frac{c_{33}}{c_{11}}, \qquad \delta_4 = \frac{c_{13}}{c_{11}}$$

4. Plane-wave propagation

We pursue the plane-wave solution of the equations of the form

$$\begin{pmatrix} u \\ w \\ T \end{pmatrix} = \begin{pmatrix} U \\ W \\ T^* \end{pmatrix} e^{i(\omega t - \xi(x\, sin\theta - z\, cos\theta))}, \tag{24}$$

$$U[\zeta_1 \xi^2 + \zeta_2] + W[\zeta_3 \xi^2 + \zeta_4] + T^* \zeta_5 = 0,$$

$$U[\zeta_6 \xi^2 - \zeta_4] + W[\zeta_7 \xi^2 + \zeta_2] + T^* \zeta_8 = 0,$$

$$\zeta_{11}\zeta_9 U + \zeta_{11}\zeta_{10} W + T^*[\zeta_{12}\xi^2 - \zeta_{11}\zeta_{13}] = 0.$$

and then eliminating U, W and T^* from the resulting equations yields the following characteristic equation

$$A\xi^6 + B\xi^4 + C\xi^2 + D = 0 \tag{25}$$

where

$$A = \zeta_1\zeta_7\zeta_{12} - \zeta_{12}\zeta_6\zeta_3,$$

$$B = \zeta_2\zeta_7\zeta_{12} + \zeta_1\zeta_2\zeta_{12} - \zeta_7\zeta_{11}\zeta_3\zeta_1 - \zeta_4\zeta_6\zeta_{12} + \zeta_3\zeta_4\zeta_{12} + \zeta_6\zeta_{11}\zeta_3^2,$$

$$C = \zeta_2^2\zeta_{12}\zeta_{25} - \zeta_2\zeta_7\zeta_{11}\zeta_3 - \zeta_2\zeta_{11}\zeta_3\zeta_1 + \zeta_4^2\zeta_{12} + \zeta_4\zeta_6\zeta_{11}\zeta_3 - \zeta_3^2\zeta_{11}\zeta_4 + \zeta_3\zeta_8\zeta_{11}\zeta_9 + \zeta_5\zeta_6\zeta_{11}\zeta_{10} - \zeta_5\zeta_{11}\zeta_9\zeta_7,$$

$$D = -\zeta_2\zeta_{11}\zeta_3\zeta_4 - \zeta_8\zeta_{11}\zeta_{10}\zeta_2 - \zeta_4^2\zeta_{11}\zeta_3 + \zeta_4\zeta_8\zeta_{11}\zeta_9 - \zeta_5\zeta_4\zeta_{11}\zeta_{10} - \zeta_5\zeta_{11}\zeta_9\zeta_2,$$

$$\zeta_1 = -sin^2\theta - \delta_2 cos^2\theta,$$

$$\zeta_2 = \left(\frac{\varepsilon_0 \mu_0^2 H_0^2}{\rho} + 1\right)\omega^2 + \Omega^2,$$

$$\zeta_3 = (\delta_4 + 1)sin\theta cos\theta,$$

$$\zeta_4 = -2\omega\Omega i,$$

$$\zeta_5 = isin\theta,$$

$$\zeta_6 = \delta_1 sin\theta cos\theta,$$

$$\zeta_7 = \delta_2 sin^2\theta - \delta_3 cos^2\theta,$$

$$\zeta_8 = -i\frac{\beta_3}{\beta_1}cos\theta,$$

$$\zeta_9 = -\beta_1^2 T_0 \omega^2 isin\theta\ ,$$

$$\zeta_{10} = \beta_1\beta_3 T_0 \omega^2 icos\theta,$$

$$\zeta_{11} = 1 + \frac{\tau_q^\alpha}{\alpha!}(i\omega)^\alpha + \frac{\tau_q^{2\alpha}}{2\alpha!}(i\omega)^{2\alpha}\ ,$$

$$\zeta_{12} = \left[1 + \frac{C_1}{L}\frac{\tau_T^\alpha}{\alpha!}(i\omega)^{\alpha+1}\right][-K_1 sin^2\theta - K_3 cos^2\theta] + \left[1 + \frac{\tau_v^\alpha}{\alpha!}(i\omega)^\alpha\right][-K_1^* sin^2\theta + K_3^* cos^2\theta],$$

$$\zeta_{13} = C_1^2 \rho C_E \omega^2$$

The roots of Eq. (25) give six roots of ξ that is, $\pm\xi_1$,$\pm\xi_2$ and $\pm\xi_3$, in which we are interested in those roots whose imaginary parts are positive. Corresponding to these roots, there exist three waves corresponding to descending order of their velocities namely a quasi-longitudinal (QL), quasi-transverse (QTS) and quasi-thermal waves (QT). The phase velocities, attenuation coefficients, specific loss and penetration depth of these waves are obtained by the following expressions.

(i) Phase velocity

The phase velocities are given by

$$V_i = \frac{\omega}{Re(\xi_i)}, \qquad \text{i} = 1, 2, 3$$

where V_1, V_2, V_3 are the velocities of QL, QTS and QT waves respectively.

(ii) Attenuation Coefficient

The attenuation coefficient is defined as

$$Q_i = Img(\xi_i), \qquad \text{i} = 1, 2, 3.$$

where Q_1, Q_2, Q_3 are the attenuation coefficients of QL, QTS and QT waves respectively.

(iii) Specific Loss

The specific loss is the ratio of energy (ΔW) dissipated in taking a specimen through a cycle, to elastic energy (W) stored in a specimen when the strain is maximum. The specific loss is the most direct method of defining internal friction for a material. For a sinusoidal plane wave of small amplitude it was shown by Kolsky (1963) that specific loss $\frac{\Delta W}{W}$ equals 4π times the absolute value of the imaginary part of ξ to the real part of ξ i.e.

$$W_i = \left(\frac{\Delta W}{W}\right)_i = 4\pi \left|\frac{Img(\xi_i)}{Re(\xi_i)}\right|, \qquad \text{i} = 1, 2, 3.$$

Where W_1, W_2, W_3 are specific loss of QL, QTS and QT waves respectively.

(iv) Penetration depth

The penetration depth is defined by

$$S_i = \frac{1}{Img(\xi_i)}, \qquad \text{i} = 1, 2, 3.$$

where S_1, S_2, S_3 are penetration depth of QL, QTS, and QT waves respectively.

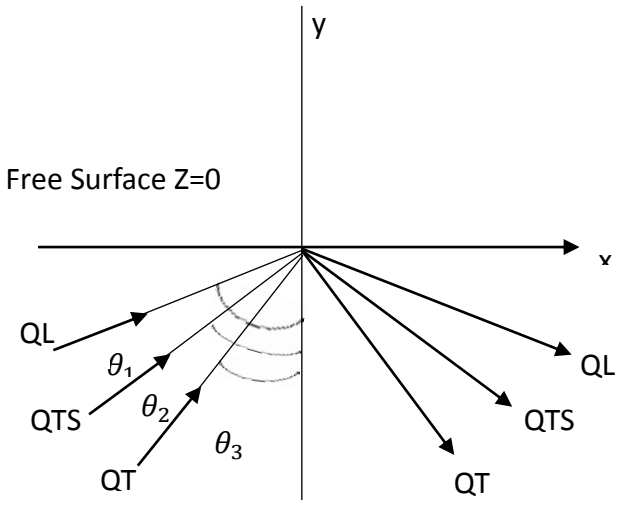

Fig. 1 Geometry of the problem

5. Reflection and transmission at the boundary surfaces

We consider a homogeneous transversely isotropic magneto thermoelastic half-space occupying the region $z \geq 0$. Incident quasi-longitudinal or quasi-transverse or quasithermal waves at the stress-free, thermally insulated surface (z = 0) will generate reflected QL, reflected QTS and reflected QT waves in the half-space z > 0. The total displacements, conductive temperature are given by

$$u = \sum_{j=1}^{6} A_j e^{iM_j},$$
$$w = \sum_{j=1}^{6} d_j A_j e^{iM_j},$$
$$T = \sum_{j=1}^{6} l_j A_j e^{iM_j}, j = 1,2,3, \dots,6 \tag{26}$$

Where

$$M_j = \omega t - \xi_j(x sin\theta_j - z cos\theta_j), j = 1,2,3,$$
$$M_j = \omega t - \xi_j(x sin\theta_j + z cos\theta_j), j = 4,5,6.$$

Here subscripts j = 1, 2, 3 respectively denote the quantities corresponding to incident QL, QTS, and QT-mode, whereas the subscripts j=4, 5, 6 denote the corresponding reflected waves, ξ_j are the roots obtained from Eq. (25).

$$d_j = \frac{-(\zeta_2\zeta_{11}\zeta_{13} + \zeta_{5j}\zeta_{11}\zeta_{9j}) + (\zeta_2\zeta_{12j} - \zeta_{11}\zeta_{13}\zeta_{1j})\xi_j^2 + \zeta_1 j\zeta_{12j}\xi_j^4}{\zeta_{7j}\zeta_{12j}\xi_j^4 + (\zeta_2\zeta_{12j} - \zeta_{7j}\zeta_{11}\zeta_{13})\xi_j^2 - (\zeta_2\zeta_{11}\zeta_{13} + \zeta_{8j}\zeta_{11}\zeta_{10j})},$$
$$\text{j} = 1,2,3.$$
$$l_j = \frac{(\zeta_2^2 + \zeta_4^2) + (\zeta_2\zeta_{1j} + \zeta_2\zeta_{7j} - \zeta_4\zeta_{6j} + \zeta_4\zeta_{3j})\xi_j^2 + \zeta_1 j\zeta_{12j}\xi_j^4}{\zeta_{7j}\zeta_{12j}\xi_j^4 + (\zeta_2\zeta_{12j} - \zeta_{7j}\zeta_{11}\zeta_{13})\xi_j^2 - (\zeta_2\zeta_{11}\zeta_{13} + \zeta_{8j}\zeta_{11}\zeta_{10j})},$$
$$\text{j} = 1,2,3.$$
$$d_j = \frac{-(\zeta_2\zeta_{11}\zeta_{13} + \zeta_{5j}\zeta_{11}\zeta_{9j}) + (\zeta_2\zeta_{12j} - \zeta_{11}\zeta_{13}\zeta_{1j})\xi_j^2 + \zeta_1 j\zeta_{12j}\xi_j^4}{\zeta_{7j}\zeta_{12j}\xi_j^4 + (\zeta_2\zeta_{12j} - \zeta_{7j}\zeta_{11}\zeta_{13})\xi_j^2 - (\zeta_2\zeta_{11}\zeta_{13} - \zeta_{8j}\zeta_{11}\zeta_{10j})},$$
$$\text{j} = 4,5,6.$$
$$l_j = \frac{(\zeta_2^2 + \zeta_4^2) + (\zeta_2\zeta_{1j} + \zeta_2\zeta_{7j} + \zeta_4\zeta_{6j} - \zeta_4\zeta_{3j})\xi_j^2 + \zeta_1 j\zeta_{12j}\xi_j^4}{\zeta_{7j}\zeta_{12j}\xi_j^4 + (\zeta_2\zeta_{12j} - \zeta_{7j}\zeta_{11}\zeta_{13})\xi_j^2 - (\zeta_2\zeta_{11}\zeta_{13} - \zeta_{8j}\zeta_{11}\zeta_{10j})},$$
$$\text{j} = 4,5,6.$$

6. Boundary conditions

The dimensionless boundary conditions at the free surface z = 0, are given by

$$t_{33} = 0 \tag{27}$$

$$t_{31} = 0 \tag{28}$$

$$\frac{\partial T}{\partial z} = 0 \tag{29}$$

Making use of Eq. (26) into the boundary conditions Eqs. (27)-(29), we obtain

$$\sum_{j=1}^{3} A_j e^{i(\omega t - \xi_j (x sin\theta_j))} \left[-C_{13} i\xi_j sin\theta_j + C_{33} i d_j \xi_j cos\theta_j - \beta_3 l_j\right] - \sum_{j=4}^{6} A_j e^{i(\omega t - \xi_j (x sin\theta_j))} \left[C_{13} i\xi_j sin\theta_j + C_{33} i d_j \xi_j cos\theta_j + \beta_3 l_j\right] = 0 \tag{30}$$

$$\sum_{j=1}^{3} A_j e^{i(\omega t - \xi_j (x sin\theta_j))} \left[\xi_j cos\theta_j - d_j \xi_j sin\theta_j\right] - \sum_{j=4}^{6} A_j e^{i(\omega t - \xi_j (x sin\theta_j))} \left[\xi_j cos\theta_j + d_j \xi_j sin\theta_j\right] = 0 \tag{31}$$

$$\sum_{j=1}^{3} A_j e^{i(\omega t - \xi_j (x sin\theta_j))} \left[i l_j \xi_j cos\theta_j\right] - \sum_{j=4}^{6} A_j e^{i(\omega t - \xi_j (x sin\theta_j))} \left[i l_j \xi_j cos\theta_j\right] = 0 \tag{32}$$

The Eqs. (30)-(32) are satisfied for all values of x, therefore we have

$$M_1(x,0) = M_2(x,0) = M_3(x,0) = M_4(x,0) = M_5(x,0) = M_6(x,0) \tag{33}$$

From Eqs. (26) and (33), we obtain

$$\xi_1 sin\theta_1 = \xi_2 sin\theta_2 = \xi_3 sin\theta_3 = \xi_4 sin\theta_4 = \xi_5 sin\theta_5 = \xi_6 sin\theta_6 \tag{34}$$

which is the form of Snell's law for stress-free, thermally insulated surface of transversely isotropic magneto thermoelastic medium with rotation. Eqs. (30)-(32) and (34) yield

$$\sum_{j=1}^{3} X_{ij} A_j + \sum_{j=4}^{6} X_{ij} A_j = 0, \quad (i = 1,2,3). \tag{35}$$

Where for p = 1, 2, 3, we have

$$X_{1p} = -C_{13} i\xi_p sin\theta_p + C_{33} i d_p \xi_p cos\theta_p - \beta_3 l_p,$$
$$X_{2p} = \xi_p cos\theta_p - d_p \xi_p sin\theta_p,$$
$$X_{3p} = i l_p \xi_p cos\theta_p.$$

And for j = 4, 5, 6 we have

$$X_{1j} = -C_{13} i\xi_j sin\theta_j - C_{33} i d_j \xi_j cos\theta_j - \beta_3 l_j,$$
$$X_{2j} = -\xi_j cos\theta_j - d_j \xi_j sin\theta_j,$$
$$X_{3j} = -i l_j \xi_j cos\theta_j.$$

Incident QL-wave

In the case of a quasi-longitudinal wave, the subscript p takes only one value, that is p=1, which means $A_2 = A_3 = 0$. Dividing the set of Eqs. (35) throughout by A_1, we obtain a system of

three homogeneous in three which can be solved by Cramer's rule and we have

$$A_{1i} = \frac{A_{i+3}}{A_1} = \frac{\Delta_i^1}{\Delta} \tag{37}$$

Incident QTS-wave

In the case of quasi-transverse wave, the subscript q takes only one value, that is p=2, which means $A_1 = A_3 = 0$. Dividing the set of Eqs. (35) throughout by we obtain a system of three homogeneous equations in three unknowns which can be solved by Cramer's rule and we have

$$A_{2i} = \frac{A_{i+3}}{A_2} = \frac{\Delta_i^2}{\Delta} \tag{38}$$

Incident QT-wave

In the case of quasi-thermal wave, the subscript q takes only one value, that is p = 3, which means $A_2 = A_1 = 0$. Dividing the set of Eq. (35) throughout we obtain a system of three homogeneous equations in three unknowns which can be solved by Cramer's rule and we have

$$A_{3i} = \frac{A_{i+3}}{A_3} = \frac{\Delta_i^3}{\Delta} \tag{39}$$

Where Z_i (i=1,2,3) are the amplitude ratios of the reflected QL, reflected QTS, reflected QT -waves to that of the incident QL-(QTS or QT) waves respectively.

Here

$$\Delta = \left|A_{i(i+3)}\right|_{3X3}$$
$$\Delta_i^p \ , (i = 1,2,3)$$

can be obtained by replacing, respectively, the 1st, 2nd and 3rd columns of Δ by $\left[-X_{1p}, -X_{2p}, -X_{3p}\right]'$

Following Achenbach (1973), the energy flux across the surface element, which is the rate at which the energy is communicated per unit area of the surface is represented as

$$P^* = t_{lm} n_m \dot{u}_l \tag{40}$$

Where t_{lm} is the stress tensor, n_m are the direction cosines of the unit normal and $\dot{u}_l$ are the components of the particle velocity.

The time average of P^* over a period, denoted $< P^* >$ represents the average energy transmission per unit surface area per unit time and is given at the interface z=0 as

$$< P^* > = < Re(t_{13}).Re(\dot{u}_1) + Re(t_{33}).Re(\dot{u}_3) > \tag{41}$$

Following Achenbach (1973), for any two complex functions f and g, we have

$$< Re(f) >< Re(g) > = \frac{1}{2} Re(f \bar{g}) \tag{42}$$

The expressions for energy ratios E_i (i=1,2,3) for reflected QL, QT, QTH-wave are given as

(i) In case of incident QL- wave

$$E_{1i} = \frac{<P^*_{i+3}>}{<P^*_1>},\ i = 1,2,3 \tag{43}$$

(ii) In case of incident QTS- wave

$$E_{2i} = \frac{<P^*_{i+3}>}{<P^*_2>},\ i = 1,2,3 \tag{44}$$

(iii) In case of incident QT- wave

$$E_{3i} = \frac{<P^*_{i+3}>}{<P^*_3>},\ i = 1,2,3 \tag{45}$$

Where$< P_i^* >$ i = 1, 2, 3 are the average energies transmission per unit surface area per unit time corresponding to incident QL, QTS, QT waves respectively and $< P_{i+3}^* >$ i = 1, 2, 3 are the average energies transmission per unit surface area per unit time corresponding to reflected QL, QTS, QT waves respectively.

7. Numerical results and discussion

To demonstrate the theoretical results and effect of rotation, relaxation time and two temperature, the physical data for cobalt material, which is transversely isotropic, is taken from Dhaliwal and Singh (1980) is given as

Quantity	Value	Unit
c_{11}	18.78×10^{10}	$Kgm^{-1}s^{-2}$
c_{12}	8.76×10^{10}	$Kgm^{-1}s^{-2}$
c_{33}	17.2×10^{10}	$Kgm^{-1}s^{-2}$
c_{13}	8.0×10^{10}	$Kgm^{-1}s^{-2}$
c_{44}	5.06×10^{10}	$Kgm^{-1}s^{-2}$
β_1	7.543×10^{6}	$Nm^{-2}deg^{-1}$
β_3	9.208×10^{6}	$Nm^{-2}deg^{-1}$
ρ	8.954×10^{3}	Kgm^{-3}
C_E	4.27×10^{2}	$jKg^{-1}deg^{-1}$
${K_1}^*$	0.04×10^{2}	$Ns^{-2}deg^{-1}$
${K_3}^*$	0.02×10^{2}	$Ns^{-2}deg^{-1}$
T_0	293	deg
α_1	2.98×10^{-5}	K^{-1}
α_3	2.4×10^{-5}	K^{-1}

The values of frequency, rotation Ω, magnetic effect H_0, are taken as 0.03,1.0, 10, respectively. The software MATLAB 8.0.4 has been used to determine the values of phase velocity, attenuation coefficient, specific loss, penetration depth, energy ratios and amplitude ratios of reflected QL, QTS and QT waves with respect to incident QL, QTS, and QT waves respectively. The variations of phase velocity, attenuation coefficients, specific loss and penetration depth with respect to frequency are shown in Figs. 2-13. The variation of magnitude of energy ratios of reflected waves subject to incident waves has been plotted in the Figs. 14-22 with respect to angle of incidence. The variation of magnitude of amplitude ratios has been plotted in the Figs. 23-31 with respect to angle of incidence. A comparison has been made to show the effect of fractional order parameter on the various quantities.

1. The black line with a square symbol represents $\alpha = 0.5$,
2. The red line with circle symbol represents to $\alpha = 1.0$,
3. The blue line with triangle symbol represents to $\alpha = 1.5$,

PHASE VELOCITY

Figs. 2-4 indicate the variations of phase velocities with respect to frequency respectively. In almost all the frequency range and for all the values of α, the phase velocity V_1, V_2, V_3 decrease however for the range $0.6 < \omega < 0.7$ the phase velocity V_2 increase somewhat and then again decreases.

ATTENUATION COEFFICIENTS

Figs. 5-7 shows the values of attenuation with respect to frequency respectively. From the graphs it is clear that for the fractional-order parameter α=0.5 the value of attenuation coefficient Q_1, Q_2, Q_3 increases continuously. For the fractional-order parameter α=0.1 the value of attenuation coefficient Q_1 decreases for the range $0.1 \leq \omega \leq 0.5$ and then increases for the rest of range. Increase in the value of attenuation coefficient Q_2 is very small for the range $0.1 \leq \omega \leq 0.6$ but for ω>0.6 the value of Q_2 increases a lot however the value of attenuation coefficient Q_3 increases but for the range $0.5 \leq \omega \leq 0.7$ the value increases very large and then comes down at the same value and then again increases for rest of the range. For the fractional-order parameter α=1.5 the value of attenuation coefficient Q_1 decreases for the range $0.1 \leq \omega \leq 0.6$ and then increases for the rest of range. Increase in the value of attenuation coefficient Q_2 is very small for the range $0.0 \leq \omega \leq 0.5$ then comes down and for ω>0.6 the value of Q_2 increases much however the value of attenuation coefficient Q_3 increases but for the range $0.0 \leq \omega \leq 0.7$ the value increases and then comes down for the range $0.7 \leq \omega \leq 0.9$and then again increases for rest of the range.

SPECIFIC LOSS

Figs. 8-10 exhibits the variations of Specific loss with respect to frequency. From the graphs, it is clear that for the fractional-order parameter α=0.5 the value of specific loss R_1decreases for the range $0.0 \leq \omega \leq 0.1$ and then increases continuously for the rest of the range. For the fractional-order parameter α=1.0 the value of specific loss R_1 decreases for the range $0.1 \leq \omega \leq 0.5$ and then increases for the $0.5 < \omega \leq 0.6$ and then again decreases for rest of the range.

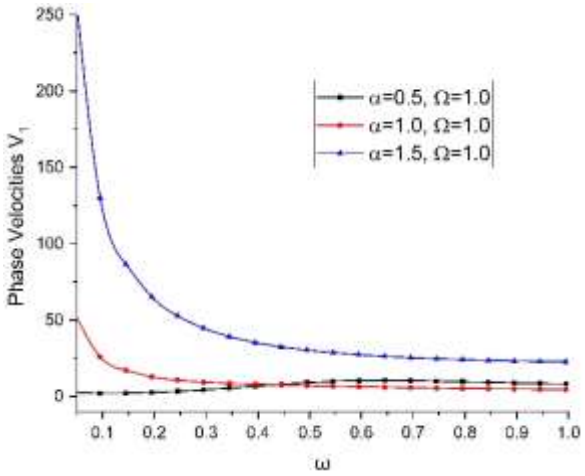

Fig. 2 Variations of phase velocity v_1 with frequency ω

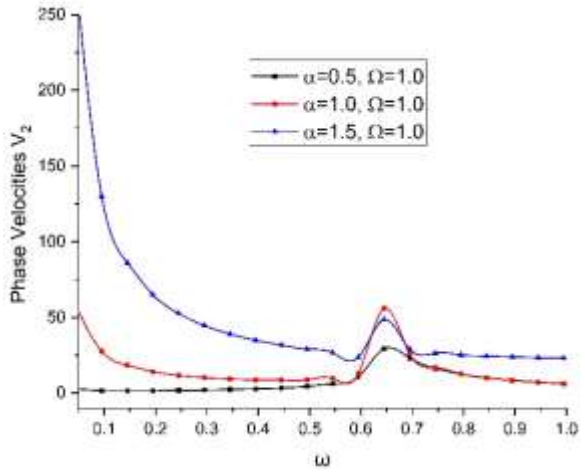

Fig. 3 Variations of phase velocity v_2 with frequency ω

Similarly for the fractional-order parameter α=1.5 the value of specific loss R_1decreases for the range $0.1 \leq \omega \leq 0.6$ and then increases for rest of the range. The value of specific loss $R_2$and R_3 shows similar variations. For the fractional-order parameter α=1.0 the value of specific loss R_2 for the range $0.5 \leq \omega \leq 0.6$ shows variation and increases sharply and then decreases and then comes down at the same value while the value of specific loss R_3 for the range $0.5 \leq \omega \leq 0.7$ shows variation and increases sharply and then decreases and then comes down at the same value for rest of the range of frequency. However For the fractional-order parameter α=1.5 the value of specific loss R_2 first remains stationary for initial range of frequency and for the range $0.5 \leq \omega \leq 0.7$ decreases somewhat and then increases for rest of the range of frequency and for α=0.5R_2 remains same for initial range and for ω>0.3 increases and the value of specific lossR_3 shows almost same variations as R_2.

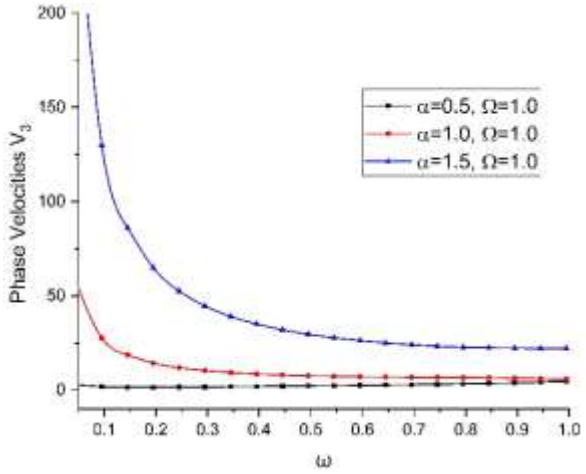

Fig. 4 Variations of phase velocity v_3 with frequency ω

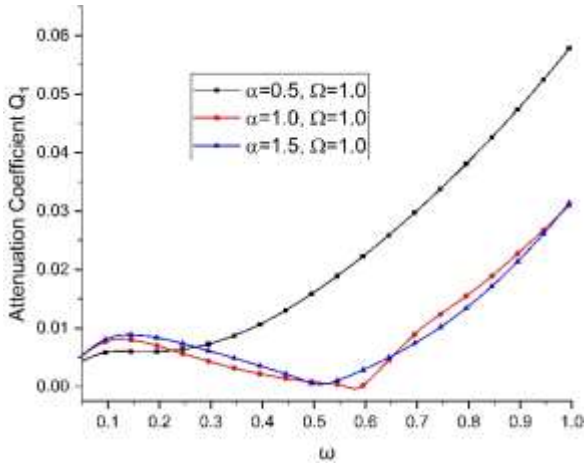

Fig. 5 Variations of attenuation coefficient Q_1 with frequency ω

PENETRATION DEPTH

Figs. 11-13 shows the variations of penetration depth S_1, S_2, S_3 with respect to frequency. Here, we notice that there is a sharp decrease in the values of S_2 and S_3 corresponding to all the cases for the range $0.0 \leq \omega \leq 0.1$,and the variations approach the boundary surface by decreasing slowly and smoothly in the rest. However, the value of penetration depthS_1, for the fractional-order parameter α=0.5 remains stationary but shows variations for $\alpha = 1.0$ and α=1.5 in the range$0.4 \leq \omega \leq 0.7$, where it increases abruptly and then comes down and remains same for rest of the range of frequency.

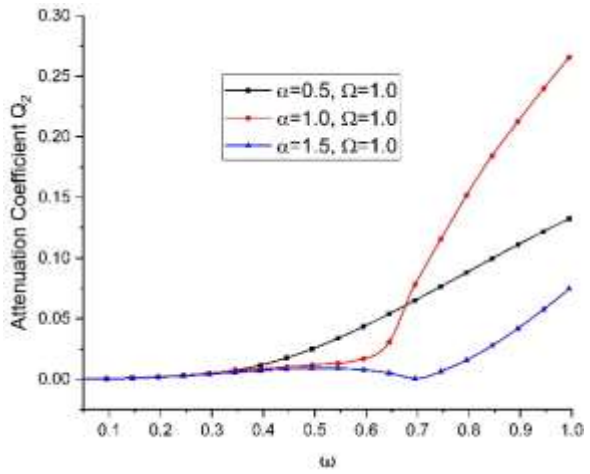

Fig. 6 Variations of attenuation coefficient Q_2 with frequency ω

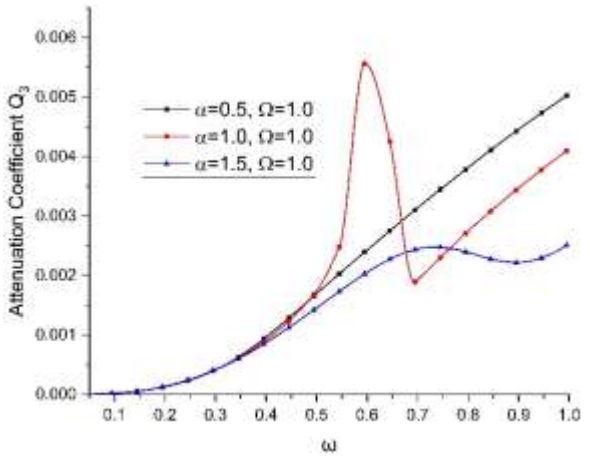

Fig. 7 Variations of attenuation coefficient Q_3 with frequency ω

ENERGY RATIOS

Incident QL wave

Fig. 14 depicts the variations of energy ratio E_{11} with respect to angle of incidence θ. It shows that the values of E_{11} decreases for the range $0 < \theta < 20$and then increases for the rest of range of angle of incidence corresponding to all the cases of fractional order parameter α. Fig. 15 shows the variations of energy ratio$E_{12}$with respect to angle of incidence θ. Here the value increases and shows same increasing pattern but difference in magnitude. Fig. 16 depicts the Variations of Energy ratio E_{13} with respect to angle of incidence θ. It is noticed that the values decrease and have variations in magnitude but not in pattern throughout the range.

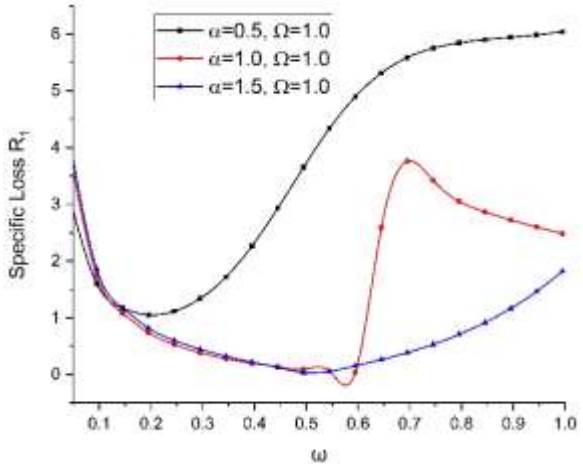

Fig. 8 Variations of specific loss R_1 with frequency ω

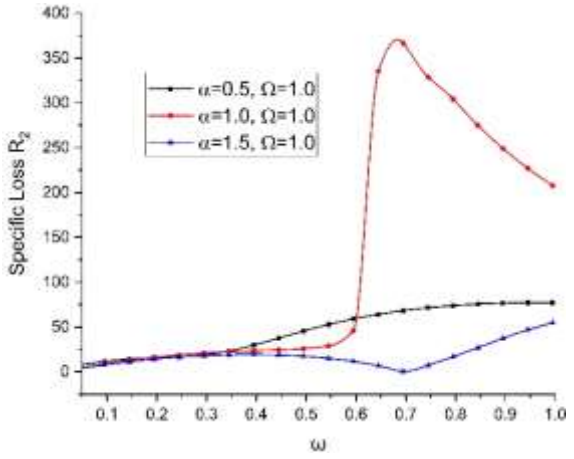

Fig. 9 Variations of specific loss R_2 with frequency ω

Incident QTS wave

Fig. 17 depicts the Variations of Energy ratio E_{21} with respect to angle of incidence θ. Here corresponding to all the cases, we notice similar increasing trends with the difference in magnitudes for the whole range and show no variation for α. Fig. 18 depicts the Variations in Energy ratio E_{22} with respect to angle of incidence θ. Here corresponding to all the cases, trends are opposite as discussed in E_{21} and shows no effect of α. Fig. 19.Variations of Energy ratioE_{23} with respect to angle of incidence θ are shown in Fig. 19. Here, we notice small variations corresponding to all the cases.E_{23} shows increasing trend with difference in magnitude with change in value of α.

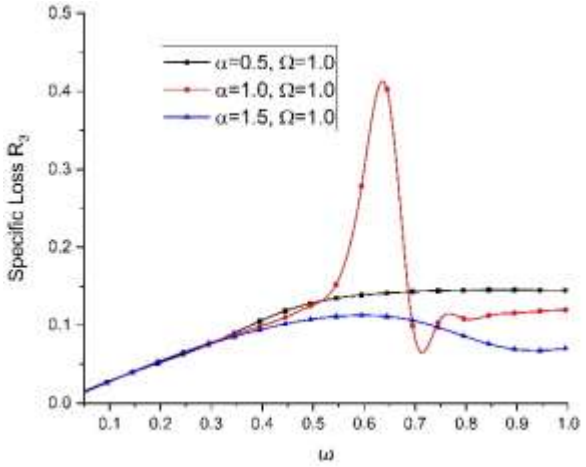

Fig. 10 Variations of specific loss R_3 with frequency ω

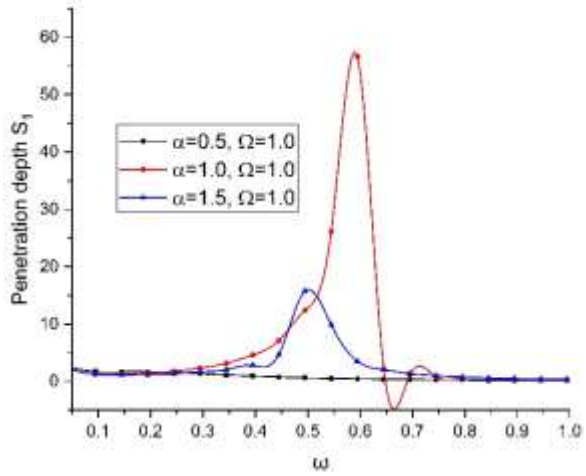

Fig. 11 Variations of penetration depth S_1 with frequency ω

Incident QT wave

Figs. 20-22 depict the Variations of Energy ratios E_{31}, E_{32}, E_{33} with respect to angle of incidence θ. Here, E_{31} and E_{33} decreases with increase in angle of incidence θ whereas E_{32} increases with increase in angle of incidence $\theta$with change in magnitude corresponding to different values of α.

AMPLITUDE RATIOS

Incident QL wave

Figs. 23-25 shows variations of amplitude ratio A_{11}, A_{12}, A_{13} with respect to the angle of incidence θ. Here, we notice that, initially, there is increase in the values of A_{11} for $\alpha =$

0.5while for $\alpha = 1.0\ and\ 1.5$ it first decreases for the initial range and then increases sharply with change in magnitude showing effect of α. The amplitude ratio A_{12} decreases with increase in angle of incidence θ and shows variations for change in value of α.Here, we notice that the values of amplitude ratio A_{13} increase monotonically for the range $0 < \theta < 30$ and after achieving maximum value at 30, the values start decreasing with difference in magnitude for $\alpha = 1.0$ and 1.5 while for $\alpha = 0.5$ it shows no variations of amplitude ratio with respect to angle of incidence θ.

Incident QT wave

Figs. 29-31 show the variations of amplitude ratios A_{31}, A_{32}, $A_{33}$with respect to the angle of incidence θ respectively. Here, the variations in Figs. 29-31 are similar as discussed in Figs. 29-31. Here, we notice that these variations show the effect of fractional order parameter α on the amplitude ratios A_{31}, A_{32}, A_{33}.

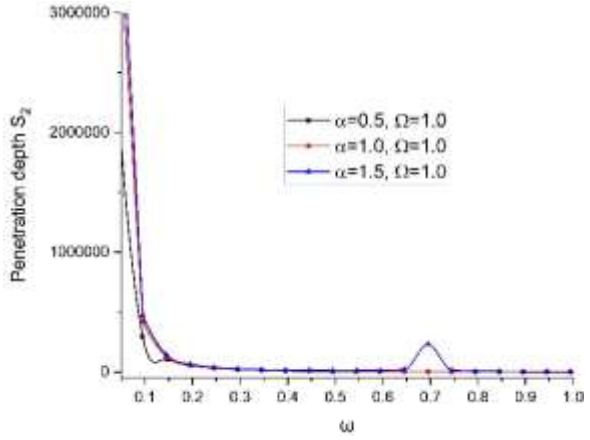

Fig. 12 Variations of penetration depth S_2 with frequency ω

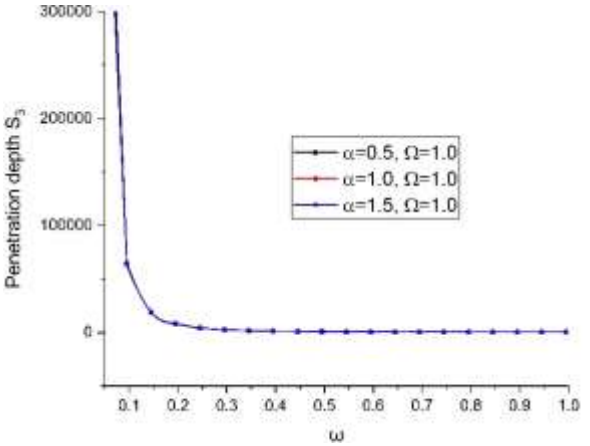

Fig. 13 Variations of penetration depth S_3 with frequency ω

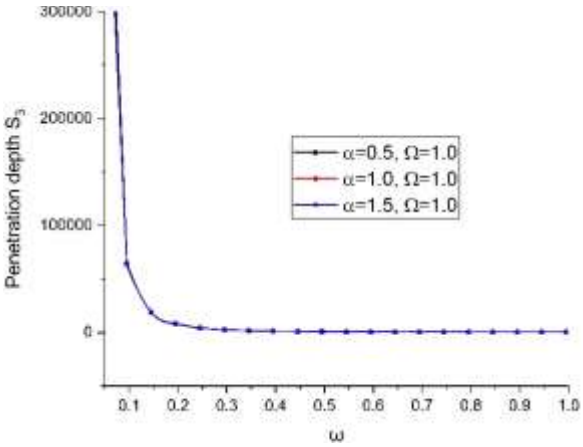

Fig. 14 Variations of energy ratio E_{11} with angle of incidence θ

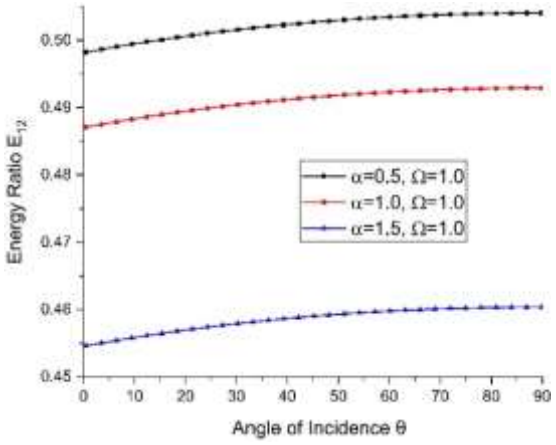

Fig. 15 Variations of energy ratio E_{12} with angle of incidence θ

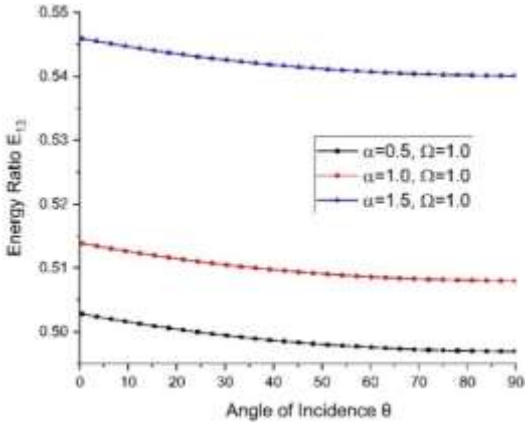

Fig. 16 Variations of energy ratio E_{13} with angle of incidence θ

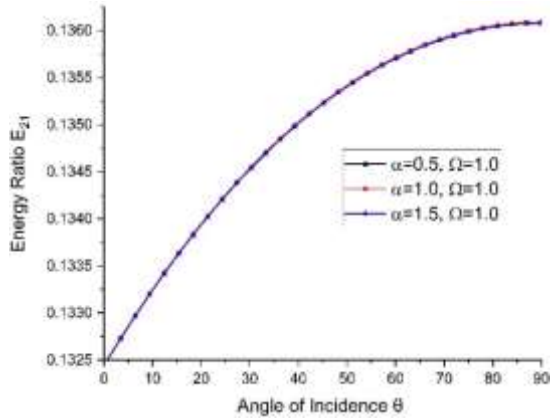

Fig. 17 Variations of energy ratio E_{21} with angle of incidence θ

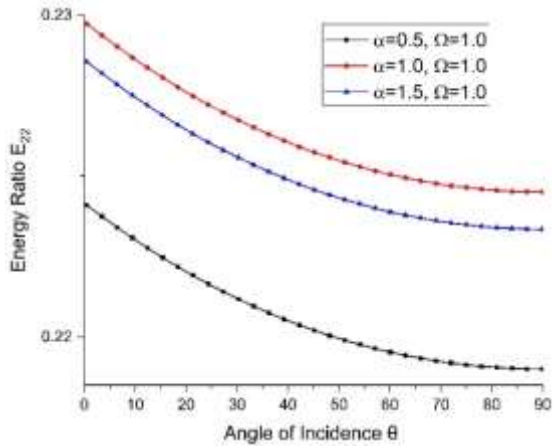

Fig. 18 Variations of energy ratio E_{22} with angle of incidence θ

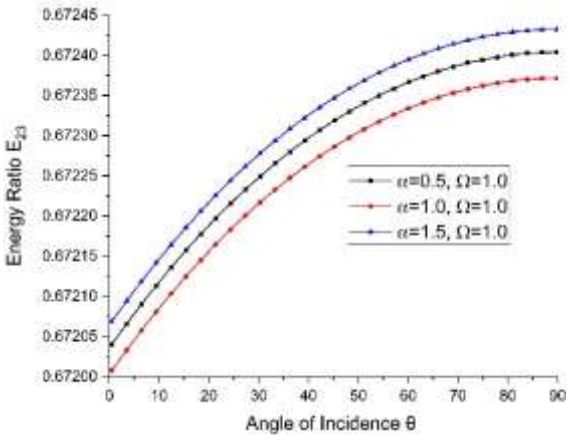

Fig. 19 Variations of energy ratio E_{23} with angle of incidence θ

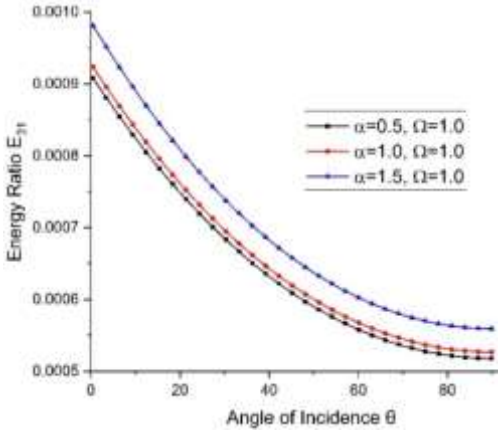

Fig. 20 Variations of energy ratio E_{31} with angle of incidence θ

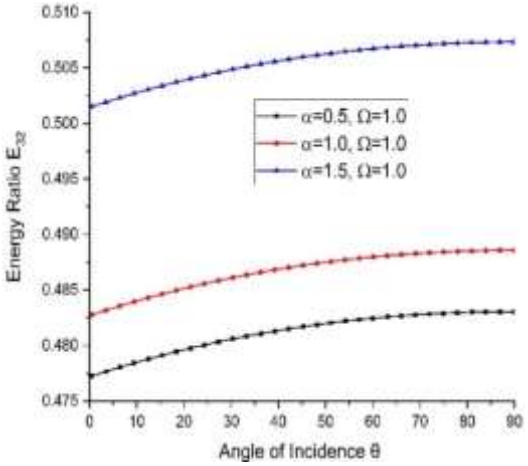

Fig. 21 Variations of energy ratio E_{32} with angle of incidence θ

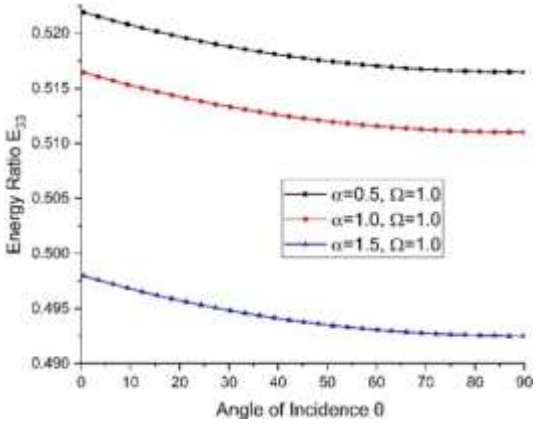

Fig. 22 Variations of energy ratio E_{33} with angle of incidence θ

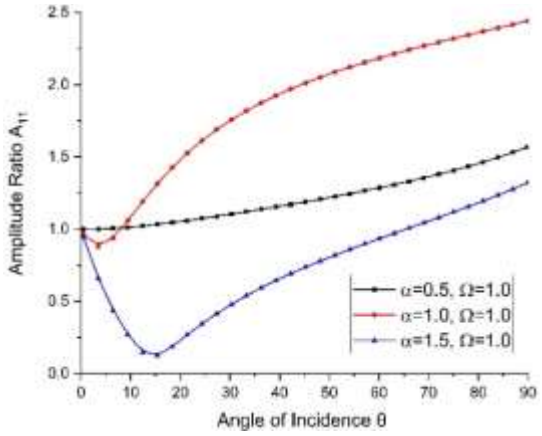

Fig. 23 Variations of amplitude ratio A_{11} with angle of incidence θ

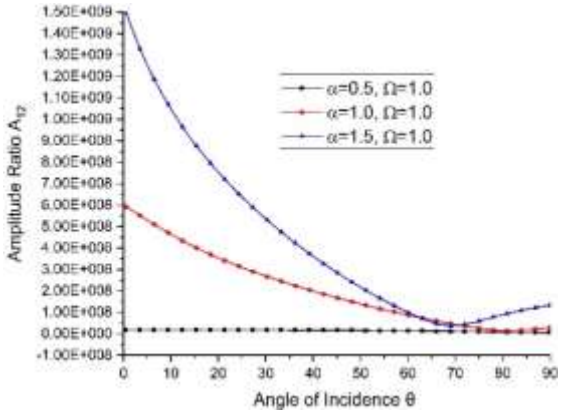

Fig. 24 Variations of amplitude ratio A_{12} with angle of incidence θ

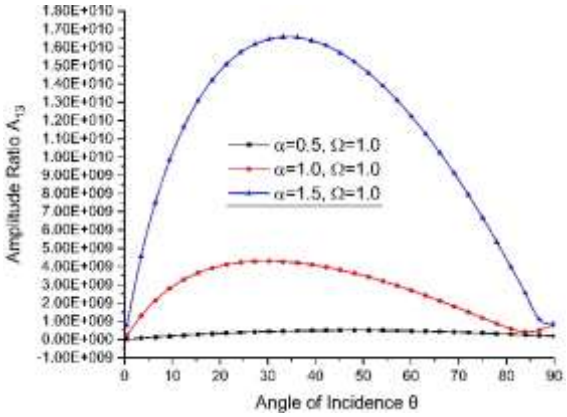

Fig. 25 Variations of amplitude ratio A_{13} with angle of incidence θ

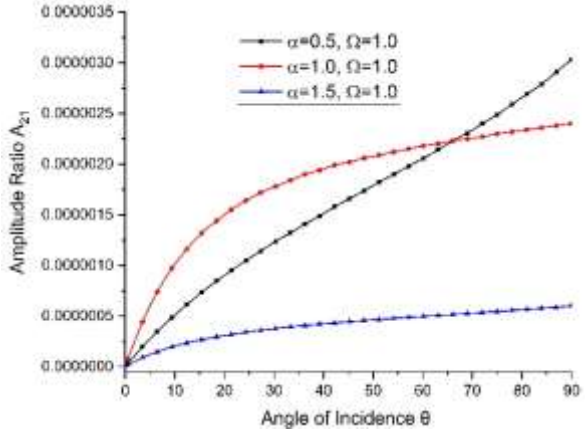

Fig. 26 Variations of amplitude ratio A_{21} with angle of incidence θ

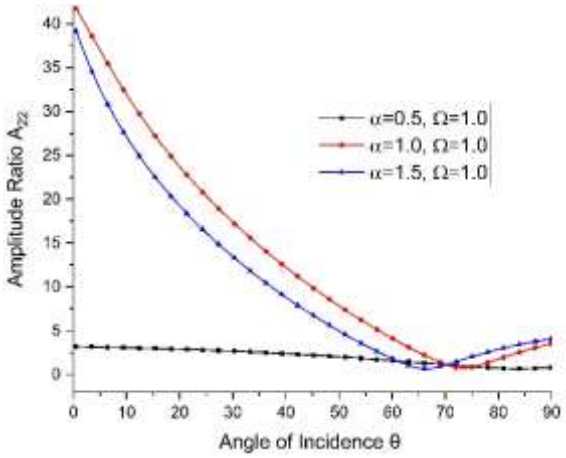

Fig. 27 Variations of amplitude ratio A_{22} with angle of incidence θ

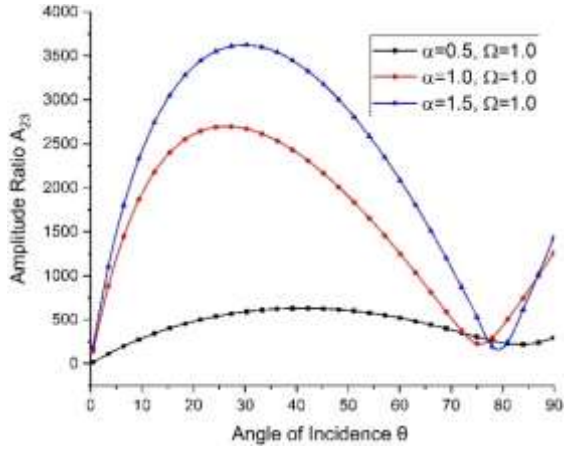

Fig. 28 Variations of amplitude ratio A_{23} with angle of incidence θ

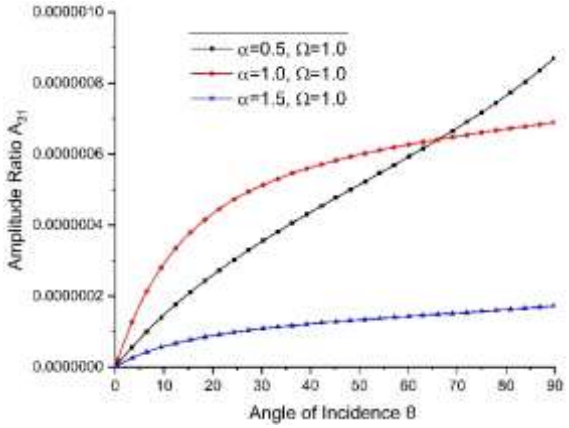

Fig. 29 Variations of amplitude ratio A_{31} with angle of incidence θ

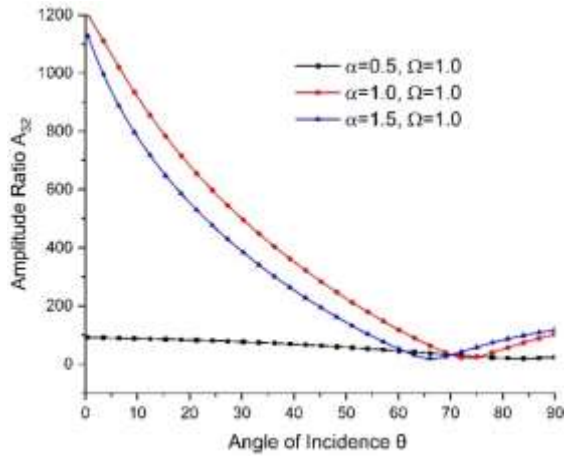

Fig. 30 Variations of amplitude ratio A_{32} with angle of incidence θ

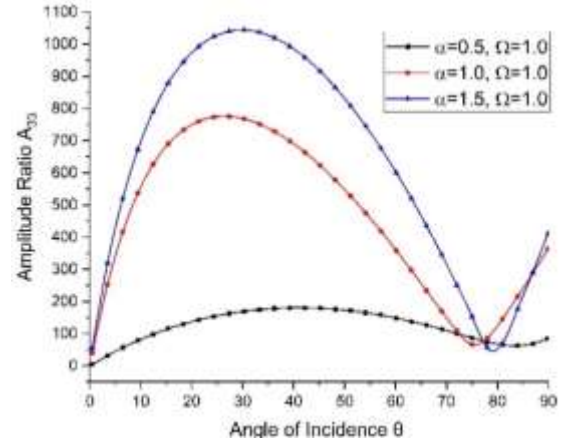

Fig. 31 Variations of amplitude ratio A_{33} with angle of incidence θ

8. Conclusions

From above investigation, we observe**:**

(i). The strong conductivity shows the major impact on the phase velocity, the weak conductivity has a high impact on the attenuation coefficients. Moreover, normal conductivity has significant impact on specific loss and penetration depth. Also, the frequency of waves formed in the material has significant effect on all the parameters of various kinds of waves.

(ii). The magnitude of energy ratios is also affected by the Fractional-order parameter and angle of incidence. As angle of incidence increases, we notice less variation in the magnitudes of energy ratios.

(iii). Fractional order parameter changes the amplitude ratios of waves. The normal conductivity when $\alpha = 1$ shows the major impact on the amplitude ratios of the waves.

(iv). The signals of these waves are not only helpful in providing information about the internal structures of the earth but also helpful in the exploration of valuable materials such as minerals, crystals, and metals, etc.

References

Abd-Alla, A.E.N.N. and Alshaikh, F. (2015), "The Mathematical model of reflection of plane waves in a transversely isotropic magneto-thermoelastic medium under rotation", *New Developments in Pure and Applied Mathematics*, 282-289.

Abouelregal, A.E. (2013), "Generalized thermoelastic infinite transversely isotropic body with a cylindrical cavity due to moving heat source and harmonically varying heat", *Meccanica*, **48**, 1731-1745.

Alesemi, M. (2018), "Plane waves in magneto-thermoelastic anisotropic medium based on (L-S) theory under the effect of Coriolis and centrifugal forces", *Proceedings of the International Conference on Materials Engineering and Applications* (pp. 01-12). IOP Conf. Series: Materials Science and Engineering.

Bayones, F. and Abd-Alla, A. (2017), "Eigenvalue approach to two dimensional coupled magneto-thermoelasticity in a rotating isotropic medium", *Results in Physics*, **7**, 2941-2949.

Borejko, P. (1996), "Reflection and transmission coefficients for three dimensional plane waves in elastic media", *Wave Motion*, **24**, 371-393.

Deswal, S. and Kalkal, K.K. (2015), "Three-dimensional half-space problem within the framework of two-temperature thermo-viscoelasticity with three-phase-lag effects", *Appl. Math. Model*., **39**, 7093-7112.

Dhaliwal, R. and Singh, A. (1980), *Dynamic coupled thermoelasticity.* New Delhi,India: Hindustan Publication Corporation.

Ezzat, M. and El-Barrry, A. (2017), " magneto-thermoelastic materials with phase-lag Green-Naghdi theories" . *Steel Compos. Struct.*, **24**(3), 297-307. doi:http://dx.doi.org/10.12989/scs.2017.24.3.297

Hassan, M., Marin, M., Ellahi, R. and Alamri, S. (2018), "Exploration of convective heat transfer and flow characteristics synthesis by Cu–Ag/water hybrid-nanofluids", *Heat Transfer Res.*, **49**(18), 1837-1848. doi:10.1615/HeatTransRes.2018025569

Kaliski, S. (1963), "Absorption of Magnetoviscoelastic surface waves in a real conductor in a magnetic field", *Proc. Vibr. Problems*, **4**, 319-329.

Kaur, I. and Lata, P. (2019b), "Effect of hall current on propagation of plane wave in transversely isotropic thermoelastic medium with two temperature and fractional order heat transfer", *SN Applied Sciences, 1:900*. doi:https://doi.org/10.1007/s42452-019-0942-1

Kaur, I. and Lata, P. (2019f), "Transversely isotropic thermoelastic thin circular plate with constant and periodically varying load and heat source", *Int. J. Mech. Mater. Eng.*, **14**(10), 1-13. doi:https://doi.org/10.1186/s40712-019-0107-4

Kumar, R. and Chawla, V. (2011), "A study of plane wave propagation in anisotropic thteephase-lag model and two-phae-lag model", *Int. Commun. Heat Mass Transfer*., **38**, 1262-1268.

Kumar, R. and Gupta, R.R. (2012), "Plane waves reflection in micropolar transversely isotropic generalized thermoelastic half-space", *Mathematical Sci*., **6**(6), 1-10.

Kumar, R. and Gupta, V. (2015),."Dual-Phase-Lag Model of Wave Propagation at the Interface between Elastic and Thermoelastic Diffusion Media", *J. Eng. Phys. Thermophys*., **88**(1), 252-265.

Kumar, R. and Kansal, T. (2017), "Reflection and Refraction of Plane HarmonicWaves at an Interface Between Elastic Solid and Magneto-thermoelastic Diffusion Solid with Voids., *Comput. Method. Sci. Technol*., **23**(1), 43-56.

Kumar, R., Sharma, N. and Lata, P. (2016), "Effects of thermal and diffusion phase-lags in a plate with axisymmetric heat supply", *Multidiscip. Model. Mater. Struct*., **12**(2), 275-290.

Kumar, R., Sharma, N. and Lata, P. (2016), "Thermomechanical interactions in transversely isotropic magnetothermoelastic medium with vacuum and with and without energy dissipation with combined effects of rotation, vacuum and two temperatures", *Appl. Math. Model*., **40**(13-14), 6560-6575.

Lata, P. (2018), "Effect of energy dissipation on plane waves in sandwiched layered thermoelastic medium", *Steel Compos. Struct*., **27**(4). doi:http://dx.doi.org/10.12989/scs.2018.27.4.439

Lata, P. (2018b), "Reflection and refraction of plane waves in layered nonlocal elastic and anisotropic thermoelastic medium", *Struct. Eng. Mech*., **66**(1), 113-124.

Lata, P. and Kaur, I. (2019a), "Transversely isotropic thick plate with two temperature and GN type-III in frequency domain", *Coupled Syst. Mech*., **8**(1), 55-70.

Lata, P. and Kaur, I. (2019c), "Thermomechanical Interactions in Transversely Isotropic Thick Circular Plate with Axisymmetric Heat Supply". *Struct. Eng. Mech*., **69**(6), 607-614. doi:http://dx.doi.org/10.12989/sem.2019.69.6.607

Lata, P. and Kaur, I. (2019d), "Transversely isotropic magneto thermoelastic solid with two temperature and without energy dissipation in generalized thermoelasticity due to inclined load", *SN Applied Sciences*, 1:426. doi:https://doi.org/10.1007/s42452-019-0438-z

Lata, P. and Kaur, I. (2019e), "Effect of rotation and inclined load on transversely isotropic magneto thermoelastic solid", *Struct. Eng. Mech*., **70**(2), 245-255. doi:http://dx.doi.org/10.12989/sem.2019.70.2.245

Lata, P., Kumar, R. and Sharma, N. (2016), "Plane waves in an anisotropic thermoelastic", *Steel Compos. Struct*., **22**(3), 567-587. doi:http://dx.doi.org/10.12989/scs.2016.22.3.567

Maitya, N., Barikb, S. and Chaudhuri, P. (2017), "Propagation of plane waves in a rotating magneto-thermoelastic fiber-reinforced medium under G-N theory", *Appl. Comput. Mech*., **11**, 47-58.

Marin, M. (1994), "The Lagrange identity method in thermoelasticity of bodies with microstructure",. *Int. J. Eng. Sci*., **32**(8), 1229-1240. doi:https://doi.org/10.1016/0020-7225(94)90034-5

Marin, M. (1997), "Cesaro means in thermoelasticity of dipolar bodies", *Acta Mechanica*, 122(1-4), 155–168.

Marin, M. (1998), "Contributions on uniqueness in thermoelastodynamics on bodies with voids", *Revista Ciencias Matematicas*, **16**(2), 101-109.

Marin, M. (1999), "An evolutionary equation in thermoelasticity of dipolar bodies", *J. Math. Phys.*, **40**(3), 1391-1399. doi:https://doi.org/10.1063/1.532809

Marin, M. (2009), "On the minimum principle for dipolar materials with stretch", *Nonlinear Anal. Real World Appl*.,**10**(3), 1572-1578.

Marin, M. (2010), "A partition of energy in thermoelasticity of microstretch bodies", *Nonlinear Analysis: Real World Appl*., **11**(4), 2436-2447.

Marin, M. and Ö chsner, A. (2017), "The effect of a dipolar structure on the Hölder stability in Green–Naghdi thermoelasticity", *Continuum Mech. Thermodyn*., **29**, 1365-1374.

Marin, M., & Craciun, E. (2017). Uniqueness results for a boundary value problem in dipolar thermoelasticity to model composite materials. *Composites Part B: Engineering, 126*, 27-37.

Marin, M., Agarwal, R.P. and Mahmoud, S.R. (2013), "Modeling a microstretch thermoelastic body with Two temperatures", *Abstract and Applied Analysis*, 2013, 1-7.

Othman, M. I. and Song, Y.Q. (2006), "The effect of rotation on the reflection of magneto-thermoelastic waves under thermoelasticity without energy dissipation", *Acta Mech*, **184**, 89-204.

Othman, M. I., Abo-Dahab, S.M. and S.Alsebaey, O.N. (2017), "Reflection of plane waves from a rotating Magneto-Thermoelastic medium with two-temperature and initial srtress under three theories", *Mechanics Mech. Eng*., **21**(2), 217–232.

Othman, M.I. and Marin, M. (2017), "Effect of thermal loading due to laser pulse on thermoelastic porous medium under G-N theory",. *Results in Physics*, 7, 3863-3872.

Othman, M.I. and Song, Y.Q. (2008), "Reflection of magneto-thermoelastic waves from a rotating elastic half-space", *Int. J. Eng. Sci*., **46**, 459-474.

Othman, M.I., Khan, A., Jahangir, R. and Jahangir, A. (2019), "Analysis on plane waves through magneto-thermoelastic microstretch rotating medium with temperature dependent elastic properties", *Appl.Math. Model*., **65**, 535-548.

Said, S.M. (2017), "A fiber-reinforced thermoelastic medium with an internal heat source due to hydrostatic initial stress and gravity for the three-phase-lag model", *Multidiscip. Model. Mater. Struct.*, **13**(1), 83-99.

Schoenberg, M. and Censor, D. (1973), "Elastic waves in rotating media", *Quarterly Appl. Math*., **31**, 115-125.

Sharma, J.N. and Kaur, R. (2015), "Modeling and analysis of forced vibrations in transversely isotropic thermoelastic thin beams", *Meccanica*, **50**, 189-205.

Sinha, S. and Elsibai, K. (1997), "Reflection and refraction of thermoelastic waves at an interface of two semi-infinite media with two relaxation times", *J. Thermal Stresses*, **20**, 129-145.

Slaughter, W.S. (2002), *The Linearised Theory of Elasticity.*, Birkhausar.

Ting, T.C. (2004), "Surface waves in a rotating anisotropic elastic half-space", *Wave Motion*, **40**, 329-346.

Wu, C. and Lundberg, B. (1996), "Reflection and transmission of the energy of harmonic elastic waves in a bent bar", *J. Sound Vib.*, **190**, 645-659.

Youssef, H. (2006), "Two-dimensional generalized thermoelasticity problem for a half space subjected to ramp -type heating.", *Eur. J. Mech. A/solid*, **25**, 745-763.

Youssef, H. (2010), "Theory of fractional order generalized thermoelasticity", *J.Heat Transfer. – ASME*, 132, 1-7.

Youssef, H.M. (2013), "State-space approach to two-temperature generalized thermoelasticity without energy dissipation of medium subjected to moving heat source",. *Appl. Math. Mech. -Engl. Ed*., **34**(1), 63-74 .

Youssef, H.M. (2016), "Theory of generalized thermoelasticity with fractional order strain", *J. Vib. Control*, ***22***(18), 3840-3857.

MK